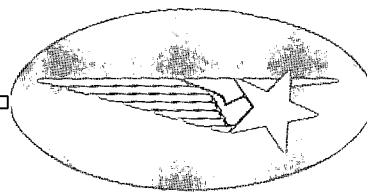


2-P (mx)



*Lockheed*

**HUNTSVILLE RESEARCH & ENGINEERING CENTER**

**LOCKHEED MISSILES & SPACE COMPANY**

A GROUP DIVISION OF LOCKHEED AIRCRAFT CORPORATION

**HUNTSVILLE, ALABAMA**

NASA-CR-124217) CALIBRATION OF PROPULSION  
SIMULATION NOZZLES FOR SPACE SHUTTLE  
BOOSTER AND ORBITER MODELS FOR THE  
ABORT/SEPARATION (Lockheed Missiles and  
Space Co.) 34 p HC \$3.75

CSCL 22B

G3/31

N73-22814

Unclas  
17580

LOCKHEED MISSILES & SPACE COMPANY  
HUNTSVILLE RESEARCH & ENGINEERING CENTER  
HUNTSVILLE RESEARCH PARK  
4800 BRADFORD DRIVE, HUNTSVILLE, ALABAMA

CALIBRATION OF PROPULSION  
SIMULATION NOZZLES FOR  
SPACE SHUTTLE BOOSTER AND  
ORBITER MODELS FOR THE  
ABORT/SEPARATION STAGING  
EXPERIMENTAL PROGRAM

July 1971

Contract NAS8-20082

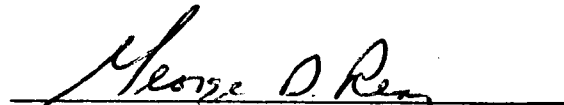
by

L. Ray Baker, Jr.

APPROVED:



John W. Benefield, Supervisor  
Fluid Mechanics Section



George D. Reny, Manager  
Aeromechanics Dept.

## FOREWORD

This document presents the results of work performed by Lockheed's Huntsville Research & Engineering Center while under subcontract to Northrop Nortronics (NSL PO 5-09287) for the Aero-Astroynamics Laboratory of Marshall Space Flight Center, Contract NAS8-20082. This task was performed in response to the requirement of Appendix B, Schedule Order 178, at the request of Mr. V. Keith Henson, S&E-AERO-AAV.

## CONTENTS

Section		Page
	FOREWORD	ii
1	INTRODUCTION AND SUMMARY	1
2	CALIBRATION TEST DESCRIPTIONS	4
	2.1 Model Nozzles	4
	2.2 Test Program	5
	2.3 Analytical Study	6
3	EXPERIMENTAL AND ANALYTICAL RESULTS	8
	3.1 Booster Nozzle	8
	3.2 Orbiter Nozzle	9
	3.3 Nozzle Setting Curve	9
4	CONCLUSIONS	12
	REFERENCES	13

Section 1  
INTRODUCTION AND SUMMARY

One of the primary areas of concern in current studies of the Space Shuttle configurations is the phenomenon surrounding the abort/separation maneuver. During this maneuver, the booster and orbiter vehicles are subjected to a combination of aerodynamic and plume gas dynamic effects, the magnitude of which are a function of vehicle orientation, trajectory conditions and vehicle main propulsion system power levels. The complexity of such a problem makes it virtually impossible to assess, analytically, the combined effects on the individual vehicles. Therefore, an experimental program was conceived to determine the power-on aerodynamic flight characteristics of the booster and orbiter vehicles during the abort separation maneuver.

An essential contribution to such a test program is the gasdynamic simulation of the size and shape of the plumes emitting from the full-scale orbiter and booster main propulsion systems. The two major effects of the plume which must be simulated are: the interaction of the plume with the external flow field, and the direct impingement of the plumes on surfaces which are enveloped by the plume. The model rocket exhaust plume will produce the correct effects on the external flow if the model plume is the correct size and shape and is in the correct location relative to the model configuration. Correct scaling of the direct impingement of the plumes on surfaces will be obtained, if in addition to the above, the model exhaust plume matches the momentum flux per unit area of the full-scale exhaust plume.

To accomplish the objective of correct plume simulation, the similarity parameters developed by Herron (Ref. 1) and the requirement to match momentum flux per unit area between the model and the full-scale systems, were applied to the orbiter and booster propulsion systems by Sims (Ref. 2). Wind tunnel facility requirements dictated the use of air or dry nitrogen ( $\gamma = 1.4$ )

as the working gas (for the model nozzles) and the use of a model sting support passing through the model base. The necessity of using a gas with a  $\gamma$  different from the full-scale system resulted in a mismatch in the momentum flux when the plume size and shape were correctly simulated. Supporting the model with a base sting system necessitated a large departure from a true scale model base for both orbiter and booster. A single annular (plug) variable area ratio conical nozzle placed concentrically around the support sting was selected as a practical means to achieve plume simulation within the constraints of the test. The similarity parameters used in the analysis were evaluated at the plume boundary. Therefore, the use of conical nozzles instead of scaled space shuttle contoured nozzles should not affect the validity of similarity parameters. In addition, it was assumed that the similarity parameters apply to plumes with boundary conditions other than quiescent air (a Newtonian pressure distribution on the plume boundary, for example. The detailed results of the simulation analysis are presented in Ref. 2.

Two plug nozzle systems have been designed and fabricated to simulate the multiple nozzle rocket exhaust plume emitting from the booster and orbiter main propulsion systems during the abort/separation maneuver. The variable area ratio capability was incorporated into both nozzle systems to permit the gasdynamic simulation of the full-scale rocket exhaust plume at the various trajectory conditions of interest.

Calibration testing of the booster and orbiter plug nozzles was accomplished in Tunnel C of the Arnold Engineering Development Center's Von Karman Gas Dynamics Facility (Ref. 3). The nozzles were tested individually at a series of area ratio settings. Nozzle operating conditions (chamber pressure,  $P_{o_j}$ , and chamber temperature,  $T_{o_j}$ ) were maintained in ranges compatible with the abort staging test conditions. A quiescent low back pressure,  $P_b$ , condition was maintained in the test cell. Data recorded at each area ratio setting included: optical data to determine plume shapes; static pressure measurements on the sting surface at the nozzle exit; nozzle mass flow measurements; and pitot pressure surveys in the plume at several axial locations downstream of the nozzle exit plane.

In a parallel effort, analytical solutions of the nozzle flow field and associated plume were generated for various area ratio settings of the booster and orbiter models. A method-of-characteristics solution employing real gas thermodynamic data for air was utilized in the calculations. Analytical results for each area ratio setting included: plume shape; static pressure distribution along sting surface; and plots of constant Mach number and constant pitot pressure contours in the plume flow field. These results formed a baseline for evaluating the experimentally measured performance of the plug nozzles.

This document presents the results of a detailed evaluation of the nozzle calibration study. A description of the test hardware is presented, and the calibration procedures are discussed. Analytical and experimental results are presented and compared.

## Section 2

### CALIBRATION TEST DESCRIPTIONS

The technical aspects of the calibration tests of the nozzles to be used in the Space Shuttle abort/separation test are discussed in this section. The model nozzles are described and the calibration test program outlined. A discussion of the analytical study conducted in support of the test program concludes this section.

#### 2.1 MODEL NOZZLES

Two "plug" nozzle systems were designed and fabricated to simulate the multiple nozzle main propulsion systems of the booster and orbiter vehicles. Each nozzle is designed so that the model vehicle support sting forms the "plug" portion of the nozzle (Fig. 1). A contoured region on each sting forms the inner nozzle wall as shown in Figs. 2 and 3. The outer wall of the nozzles is formed by a sleeve contoured internally. The contoured regions on the sting and sleeve form a contoured converging/diverging axisymmetric "plug" nozzle. The sleeve is moved fore and aft axially to change the effective throat area and thereby change the nozzle area ratio.

A desired nozzle area ratio is obtained by adjusting the outer sleeve to give the correct axial dimension,  $E_p$ , between the nozzle lip and the surface of a reference block. The reference block location is fixed on the sting surface by a reference pin (Figs. 4 and 5).

The working gas for the nozzles is room temperature air. The air is introduced into the nozzle chambers through supply lines that are integral to the model support sting. Total pressure of the air,  $P_{oj}$ , was varied over a range of 400 to 1300 psia during the test.



Actual nozzle dimensions were established by a post-test inspection conducted by personnel of the MSFC Manufacturing Engineering Laboratory. These dimensions are presented in Fig. 4 for the booster nozzle and Fig. 5 for the orbiter nozzle. In addition, nominal dimensions for each of the nozzles are included on each of the figures for comparison purposes. The location of the static pressure port and the reference pin for setting nozzle area ratio is also specified on each figure.

## 2.2 TEST PROGRAM

Calibration testing of the booster and orbiter "plug" nozzles was accomplished in Tunnel C of the Arnold Engineering Development Center's Von Karman Gas Dynamic Facility. The objectives of the nozzle calibration test were:

- Establish, experimentally, nozzle performance characteristics for the range of area ratio settings to be used with the booster and orbiter nozzles, respectively.
- Establish a curve (based on experimental results) of nozzle exit conditions as a function of nozzle area ratio setting.

Each nozzle was tested at a series of area ratio settings. The test procedure consisted of flowing high pressure ambient temperature air through the nozzle. Data recording was then initiated after continuous, steady flow was established in the nozzle. Nozzle operating conditions (chamber pressure,  $P_{0j}$ , and chamber temperature,  $T_{0j}$ ) were maintained in ranges compatible with the abort staging test conditions. Tunnel C was operated as an evacuated test cell. A quiescent, low pressure,  $P_b$ , condition was maintained in the tunnel during the test program. A summary of test conditions for the booster and orbiter nozzles is presented in Table 1.

The data recorded at each area ratio setting included:

- Holographic interferograms for determining initial plume boundary angle and plume shape

- Static pressure measurements on the sting surface at the nozzle exit
- Mass flow rate in nozzle supply line using venturi measuring system
- Pitot pressure surveys in the plume at specified axial locations downstream of the nozzle exit plane
- Nozzle total conditions,  $P_{o_j}$  and  $T_{o_j}$
- Test cell ambient pressure,  $P_b$ .

### 2.3 ANALYTICAL STUDY

An analytical study of the booster and orbiter "plug" nozzle configurations was conducted parallel with preparations for calibration test program. The objectives of this study were to: (1) establish a baseline for evaluating the experimental results; (2) provide preliminary information on nozzle performance characteristics such as thrust and mass flow rate that might affect hardware design; and (3) provide a rapid means for determining nozzle performance characteristics (if reasonable agreement is obtained between analytical and experimental results).

The initial analytical study was conducted using nominal dimensions (see Figs. 4 and 5) for the booster and orbiter nozzles. Prior to calculating nozzle performance, it was necessary to determine the variations of nozzle area ratio with nozzle setting. This was accomplished by calculating the minimum geometric throat area for each nozzle setting using an automated technique. The variation of area ratio with nozzle setting are presented in Fig. 6 for the booster nozzle and Fig. 7 for the orbiter nozzle. This information was used to determine nozzle settings for both the calibration tests and the analytical study.

Nozzle performance characteristics and internal and plume flow field properties were calculated using Lockheed's variable mixture ratio method-of-characteristics (VOFMOC) program, Ref. 4. The program was modified

to internally shift the nozzle walls to the correct relative position for a specified nozzle setting (i.e., area ratio). Real gas thermodynamic properties of air were utilized in the flowfield calculations. The gas properties were calculated from equations derived from the Beattie-Bridgeman equation of state assuming variable specific heats, Ref. 5. Flowfield calculations were initiated from the previously calculated location of the geometric throat using a constant Mach number start line. Results of these calculations are presented in Figs. 8 through 11.

Following the calibration test program, the analytical calculations were repeated using actual measured dimensions of the booster and orbiter nozzles. This information is also presented in Figs. 8 through 11.

A detailed discussion of the results of the analytical and experimental studies is presented in the following section.

### Section 3

## EXPERIMENTAL AND ANALYTICAL RESULTS

The nozzle performance characteristics of the booster and orbiter nozzles were evaluated on the basis of comparison of analytical and measured values of mass flow rate, nozzle pressure ratio, nozzle chamber pressure, and plume shape information. The experimental and analytical results were correlated on the basis of nozzle setting,  $E_p$ . Nozzle setting is defined as the measured gap between the nozzle exit lip and the surface of a reference block that is mounted on the sting during the setting operation. Actual setting of a specific nozzle gap dimension was accomplished with the use of standard gage blocks ("Jo" blocks) to within  $\pm 0.0005$  in. Figures 6 and 7 show that nozzle area ratio is extremely sensitive to the setting gap, especially for the orbiter. Also it is evident from these figures that nozzle dimensions significantly affect the distribution of area ratio with nozzle setting. The degree of success in obtaining agreement between experimental and analytical results was hinged directly on actual knowledge of the nozzle dimensions.

### 3.1 BOOSTER NOZZLE

Performance characteristics of the booster nozzle are presented in Figs. 8 and 10. The experimental and analytical mass flow rate values shown in Fig. 8 have been adjusted to a common chamber pressure,  $P_{0j}$ , base of 1000 psia for the purpose of comparison. Nozzle pressure ratio data were determined from the ratio of the static pressure,  $p_j$ , on the sting surface at the nozzle exit plane to the nozzle chamber pressure.

In general, both the mass flow and pressure ratio data suggest that the booster nozzle operates at a lower area ratio experimentally for a specific nozzle setting than it does analytically. The analytical results obtained with the measured nozzle dimensions did, however, shift closer to the experimental

results. These calculations were run with the same gasdynamic chamber conditions ( $P_{o_j}$ ,  $T_{o_j}$ ) that were measured experimentally. A comprehensive review of both sets of data revealed no gasdynamic explanation for the differences in the test and analytical results.

Because of the difficulty in measuring the nozzle contours, it is suspected that the actual nozzle dimensions are still not known. In addition, the inspection results showed that the reference block dimensions and the distance between reference pin location and nozzle lip at the "reference" condition vary from the norm enough to contribute to a lack in certainty of the knowledge of the variation of nozzle area ratio with actual gap setting.

### 3.2 ORBITER NOZZLE

Performance characteristics of the orbiter nozzle are presented in Figs. 9 and 11. These data were prepared in the same manner as they were for the booster nozzle data.

Comparison of the analytical and experimental results for the orbiter nozzle revealed a different trend than was encountered with the booster nozzle. The initial analytical results (based on nominal nozzle dimensions) fell well below the experimental results for both mass flow rate and nozzle pressure ratio. Nozzle performance calculations made using measured nozzle dimensions and calibration test gasdynamic operating conditions were above the experimental data curves but followed, in general, the contour of the experimental data curve. These results indicate again the dependency of the analytical calculation of nozzle performance on quality of the knowledge of the nozzle dimensions. As with the booster, no gasdynamic explanation of the differences in the experimental analytical results could be determined.

### 3.3 NOZZLE SETTING CURVE

The disagreement between the experimental and analytical results negated use of the analytical results to obtain nozzle setting for the abort staging test.

Therefore, experimental data were used exclusively to determine the required setting curves of nozzle lip Mach number as a function of the nozzle setting. The basic equations used to determine the desired data can be found in most gasdynamic texts.

Initially, the Mach number of the limiting Prandtl-Meyer fan is calculated from the following relation:

$$M_2 = \left\{ \left[ \left( \frac{P_{o_j}}{P_b} \right)^{\frac{\gamma_2-1}{\gamma_2}} - 1.0 \right] \frac{2}{\gamma_2-1} \right\}^{1/2} \quad (1)$$

where:  $\frac{P_{o_j}}{P_b}$  is ratio of the ambient back pressure,  $P_b$ , to the chamber pressure,  $P_{o_j}$ . Using this Mach number and the nozzle half angle,  $\theta_N$ , the resulting turning angle of the flow,  $\nu_2$  is calculated from the following equation:

$$\nu_2 = \left( \frac{\gamma_2+1}{-1} \right)^{1/2} \arctan \left[ \frac{\gamma_2-1}{\gamma_2+1} (M_2^2 - 1) \right]^{1/2} - \arctan \left( (M_2^2 - 1)^{1/2} \right) \quad (2)$$

To complete the calculations, the initial plume expansion angle,  $\delta_j$ , was determined from the experimental optical data. Examples of these data, holographic interferograms, are shown in Figs. 12 and 13 for the booster and orbiter, respectively. Values of  $\delta_j$  were obtained by measuring the initial plume angle directly from the photographs. This information was then used to obtain one expression for the flow turning angle at the nozzle lip

$$\nu_1 = \nu_2 - \delta_j \quad (3)$$

A second expression for  $\nu_1$  was then written as,

$$\nu_1 = \left( \frac{\gamma_1 + 1}{\gamma_1 - 1} \right)^{1/2} \arctan \left\{ \left[ \frac{\gamma_1 - 1}{\gamma_1 + 1} (M_1^2 - 1) \right]^{1/2} \right\} - \arctan \left[ (M_1^2 - 1) \right]^{1/2} \quad (4)$$

Combining Eqs. (3) and (4), a function was formed from which the Mach number at the nozzle lip could be calculated using iterative techniques.

$$F(M_1) = \left( \frac{\gamma_1 + 1}{\gamma_1 - 1} \right)^{1/2} \arctan \left\{ \left[ \frac{\gamma_1 - 1}{\gamma_1 + 1} (M_1^2 - 1) \right]^{1/2} \right\} - \arctan \left[ (M_1^2 - 1) \right]^{1/2} - (\nu_2 - \delta_j) \quad (5)$$

The results of these calculations are presented in Figs. 14 and 15 for the booster and orbiter, respectively. The curve for the booster was faired through data that were generally representative of the norm of the nozzle operating conditions. The orbiter data were faired through the points associated with high chamber pressures. This was done to account for the flexing of the nozzle structure which was noted at these pressures and because the high pressure was representative of most of the abort staging test conditions. These curves were utilized with plume scaling information of Ref. 2 to obtain the nozzle settings shown in Table 2.

Section 4  
CONCLUSIONS

The following conclusions were reached during the course of the nozzle calibration study:

- The use of the concept of variable area ratio nozzles for this application is sound and provides a means to satisfy plume gasdynamic simulations over a wide range of conditions.
- The ability to predict analytically the performance of nozzles of this design and size is associated directly with accurate knowledge of the nozzle dimensions.
- Although, neither the booster nor the orbiter nozzles operated precisely as anticipated, the variable area ratio capability permitted the simulation criterion to be satisfied.



## REFERENCES

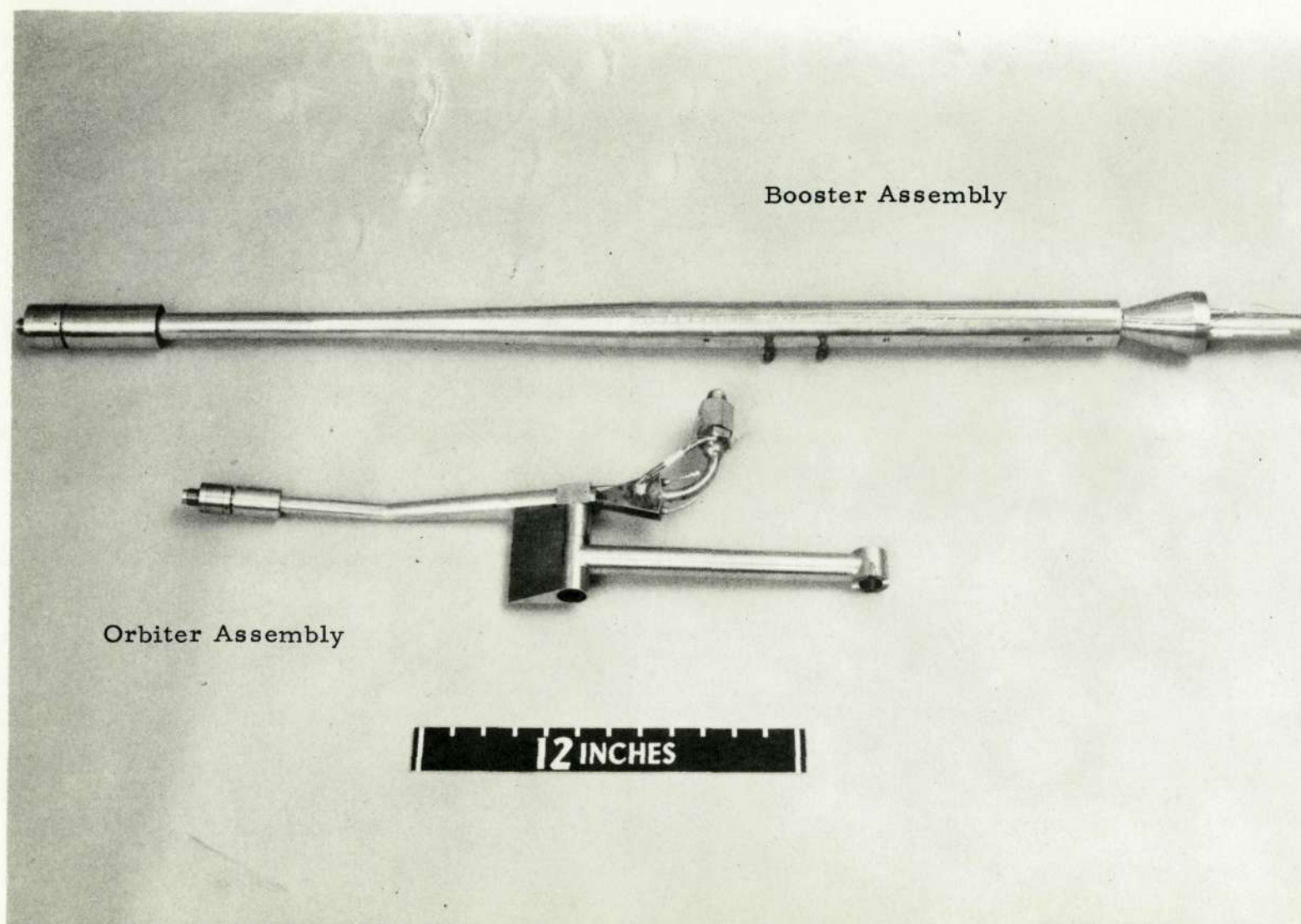
1. Herron, R. D., "Investigation of Jet Boundary Simulation Parameters for Underexpanded Jets in a Quiescent Atmosphere," AEDC TR-68-108, Arnold Air Force Station, Tenn., September 1968.
2. Sims, Joseph L., "Plume Simulation for Space Shuttle Abort Staging Aerodynamic Testing," NASA-MSFC S&E-AERO-AF-70-6, 16 December 1970.
3. Test Facilities Handbook, 8th ed., Arnold Engineering Development Center, Arnold Air Force Station, Tenn., December 1969.
4. Smith, S. D., and A. W. Ratliff, "User's Manual - Description of the Variable O/F Ratio Method-of-Characteristics Program for Nozzle and Plume Analysis," LMSC-HREC D162220-I, Lockheed Missiles & Space Company, Huntsville, Ala., July 1971.
5. Randall, R. E., "Thermodynamic Properties of Gases: Equations Derived from the Beattie-Bridgeman Equation of State Assuming Variable Specific Heats," AEDC TR-57-10, Arnold Air Force Station, Tenn., August 1957.

Table 1  
TEST CONDITIONS FOR SPACE SHUTTLE NOZZLE  
PLUME CALIBRATION TEST

Run/Group	Configuration	Nom. M	P <sub>b</sub> (psia)	T <sub>o</sub> (°F)	E <sub>p</sub> (in. )	P <sub>oj</sub> (psia)	Inter- fero- gram	Rake Sta. (in. )
1	Booster	0	0.36	100	0.389	505	X	
2			↓		↓	640	X	
3			↓		↓	↓		
4			0.40		↓	↓		
5			0.40		↓	↓	X	
6			0.33		0.411	500	X	
7			↓		↓	460	X	
8			↓		↓	550		
9			0.34		↓	550		
10			0.31		0.426	430	X	
11			0.33		↓	572		
12			↓		↓	↓	X	
13			↓		↓	↓	X	
13			↓		↓	660	X	
13			↓		↓	250	X	
14			0.26		0.542	450	X	
15	Booster	0	↓	↓	↓		2.28	
16			0.26	0.542	405	X	0.71	
17			0.33	0.592	330	X		
18			↓	↓	430	X	0.71	
19			0.33	↓	1200	X		
20			0.28	0.452	390	X		
21			↓	↓	485	X	1.52	
22			↓	↓	485		0.71	
23			0.28	0.504	485		0.71	
24			↓	↓	485	X	1.52	
25			↓	↓	430	X		
26	Orbiter		0.26	0.478	415		0.47	
27			↓	↓	↓	X	0.94	
↓			↓	↓	800	X		
↓			↓	↓	1200	X		
28			↓	0.512	415		0.47	
29			↓	↓	↓	X	0.94	
29			↓	↓	800	X		
29			Orbiter Orbiter	0	0.512	1240	X	
30				0	0.545	1200	X	
↓				↓	↓	800	X	
↓				↓	↓	415	X	
31				↓	0.495	415	X	0.47
↓				↓	↓	800	X	
↓				↓	↓	1200	X	
↓	↓	↓		↓	X			

Table 2  
NOZZLE SETTINGS FOR SPACE SHUTTLE  
ABORT SEPARATION TEST PROGRAM

Thrust Level		Mach No.	Altitude (ft)	Booster		Orbiter	
Booster (%)	Orbiter (%)			$E_p$ (in.)	$P_s/P_c$	$E_p$ (in.)	$P_s/P_c$
0	0	5	153,000	—	—	—	—
0	0	2	60,500	—	—	—	—
0	0	2	60,500	—	—	—	—
50	100	2	60,500	.560	.0115	.502	.00548
0	0	3	93,700	—	—	—	—
50	100	3	93,700	.519	.0172	.485	.00754
0	0	5	153,000	—	—	—	—
50	100	5	↓	.491	.0218	.471	.01024
0	100	5		—	—	.471	.01024
100	100	5		.473	.0251	.471	.01024
50	50	5		.491	.0218	.473	.00974
0	0	5		—	—	—	—
50	100	5		.491	.0218	.471	.01024
0	0	5		—	—	—	—
50	100	5	60,500	.491	.0218	.471	.01024
0	0	2	↓	—	—	—	—
0	↓	2		—	—	—	—
0		2	93,700	—	—	—	—
0		3	93,700	—	—	—	—
0		5	153,000	—	—	—	—
100		2	60,500	.522	.0167	—	—
100		3	93,700	.495	.0211	—	—
100		5	153,000	.473	.0251	—	—
0		2	60,500	—	—	—	—
0		3	93,700	—	—	—	—
0		5	153,000	—	—	—	—
100		2	60,500	.522	.0167	—	—
100		3	93,700	.495	.0211	—	—
100	0	5	153,000	.473	.0251	—	—



Orbiter Assembly

Booster Assembly

Fig. 1 - Nozzle and Sting Assemblies for the Booster and Orbier Models



Fig. 2 - Booster Nozzle Components



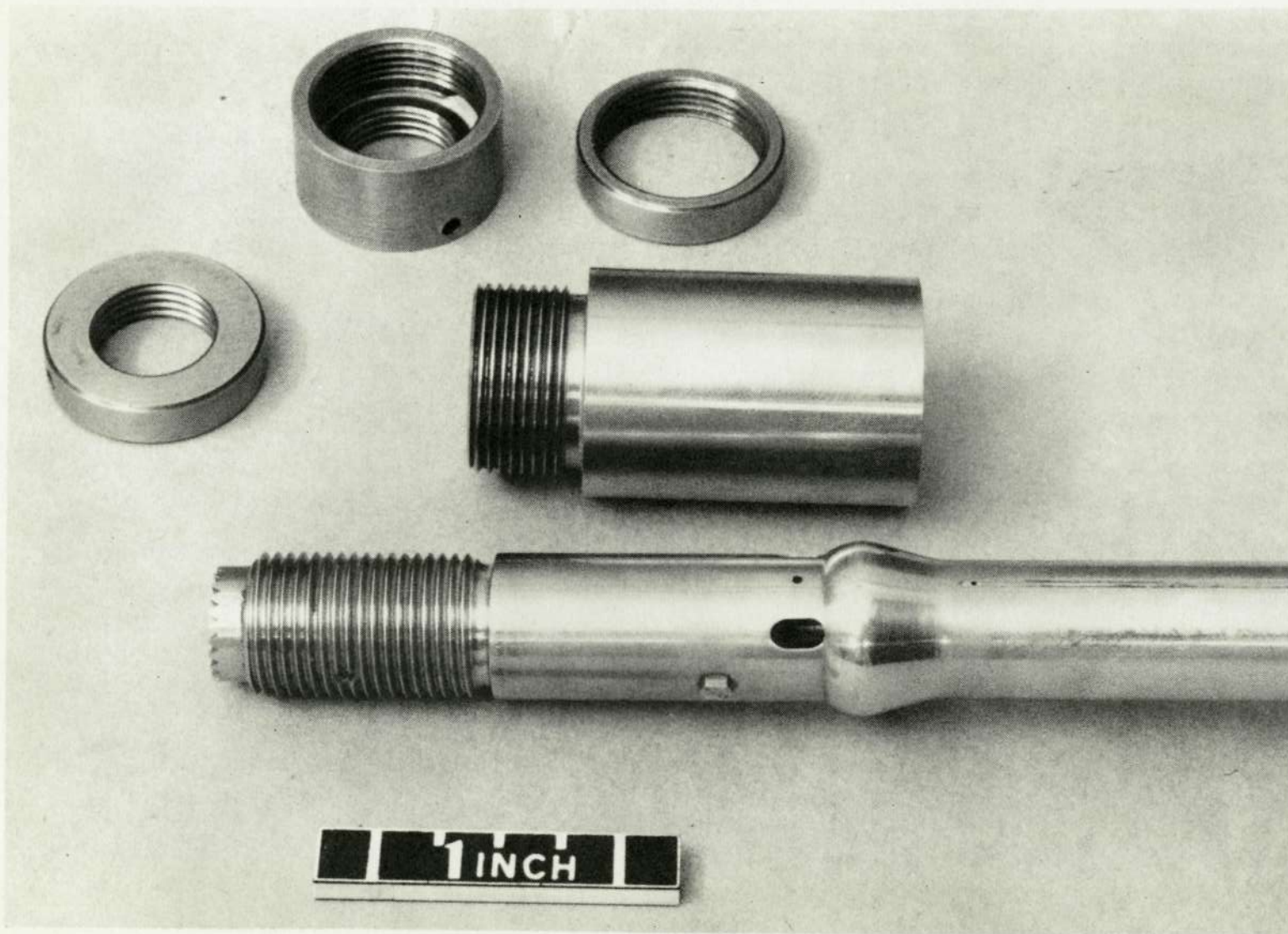
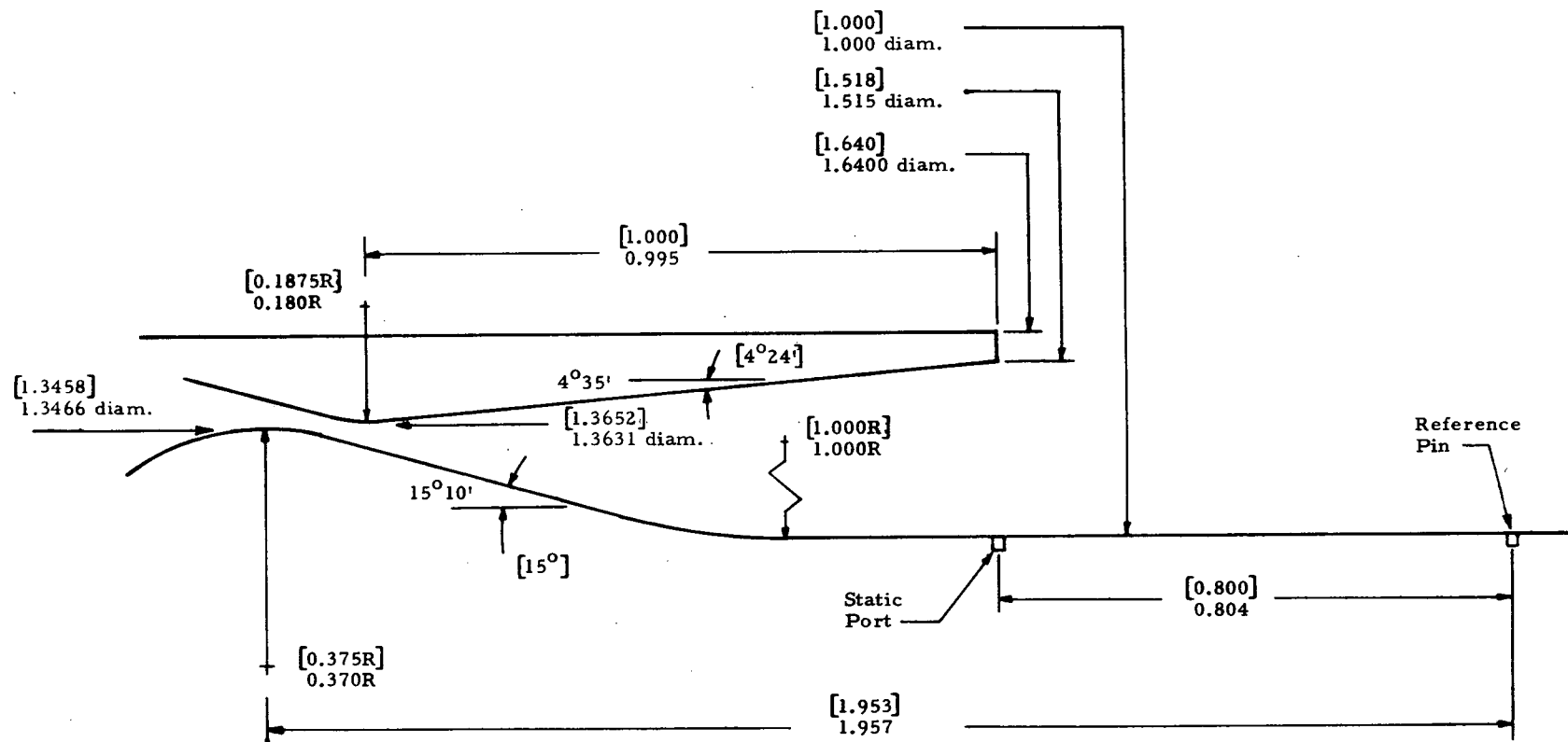
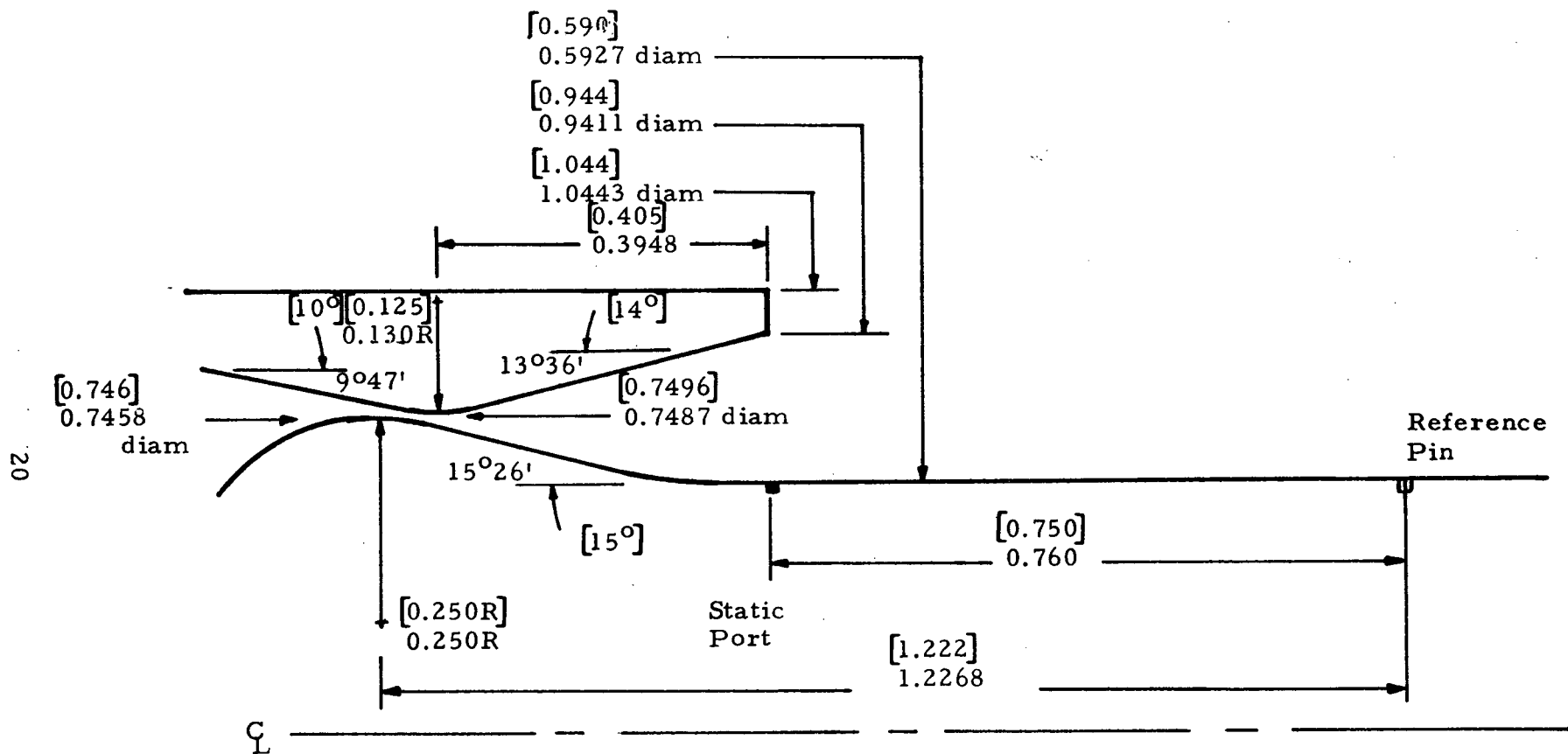


Fig. 3 - Orbiter Nozzle Components



- Notes: 1. Linear dimensions are in inches; angles are in degrees and minutes.  
 2. Dimensions in brackets, [ ], are nominal values per print LD-518401

Fig. 4 - Dimensions of Booster Nozzle Assembly as Determined by Detailed Inspection



Note: (a) Linear dimensions are in inches; angles are in degrees and minutes.  
 (b) Dimensions in brackets [ ] are nominal values per print LD-518400

Fig. 5 - Dimensions of Orbiter Nozzle Assembly as Determined by Detailed Inspection



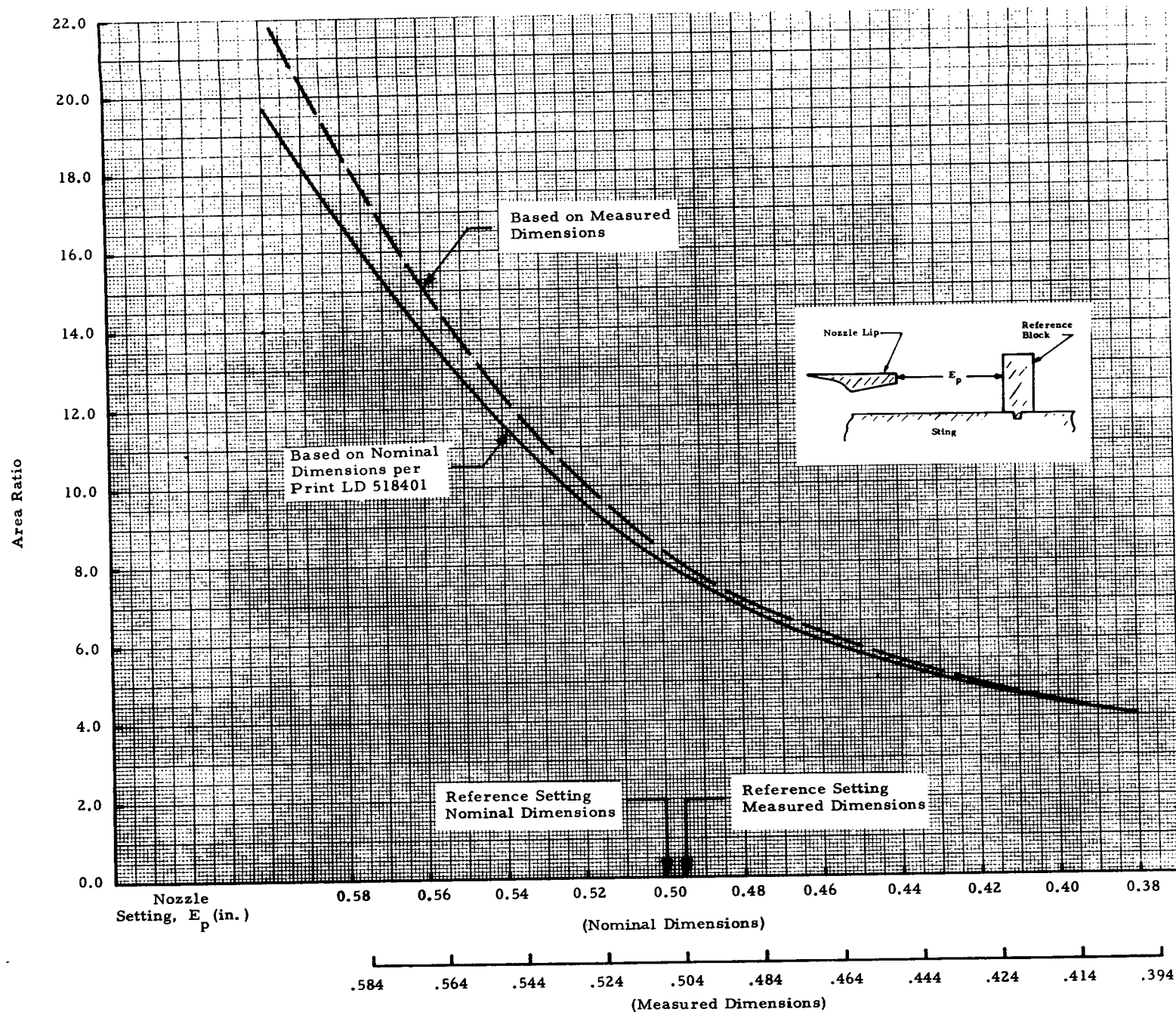


Fig. 6 - Area Ratio of Booster Nozzle as a Function of Nozzle Setting

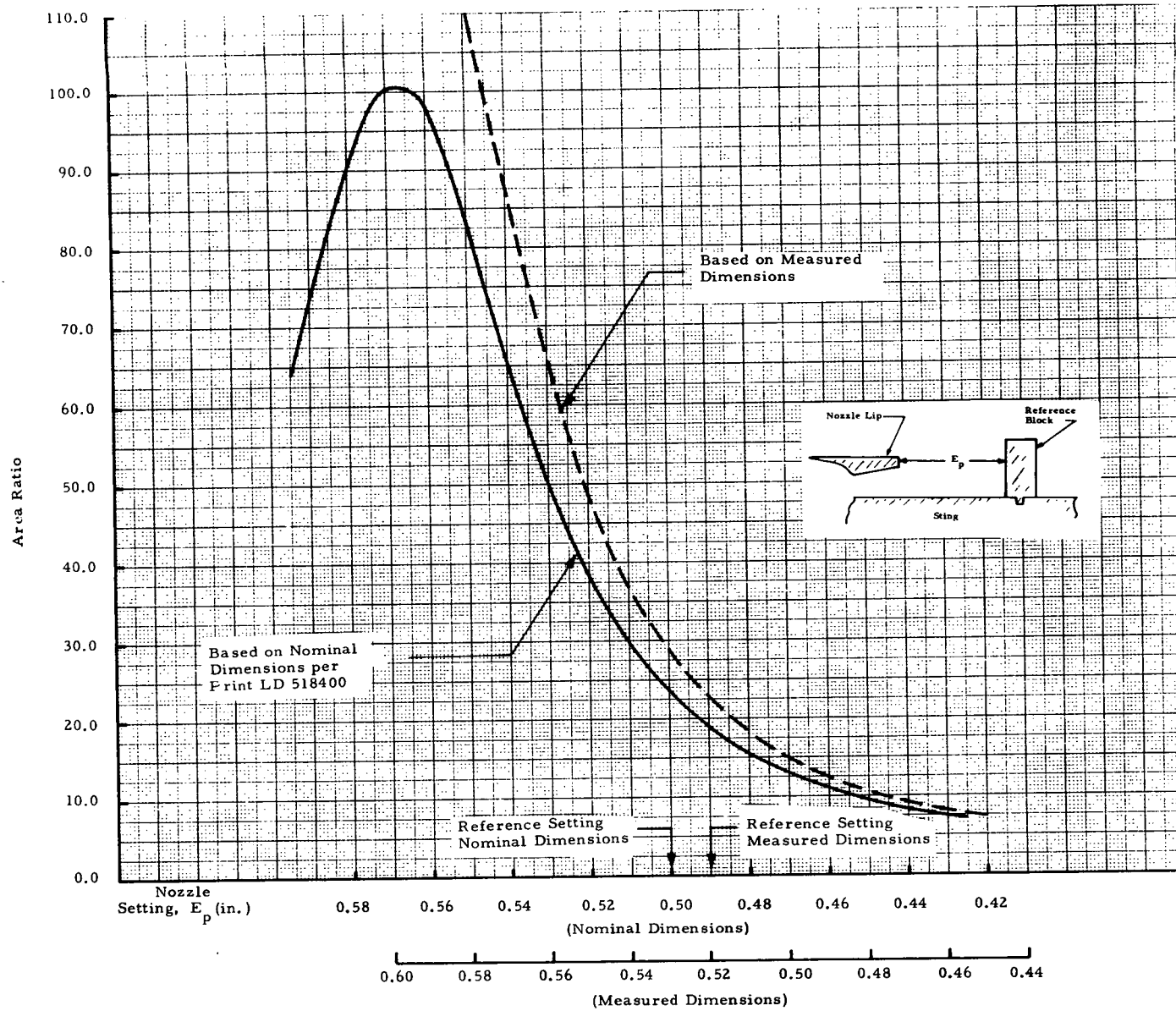


Fig. 7 - Area Ratio of the Orbiter Nozzle as a Function of Nozzle Setting

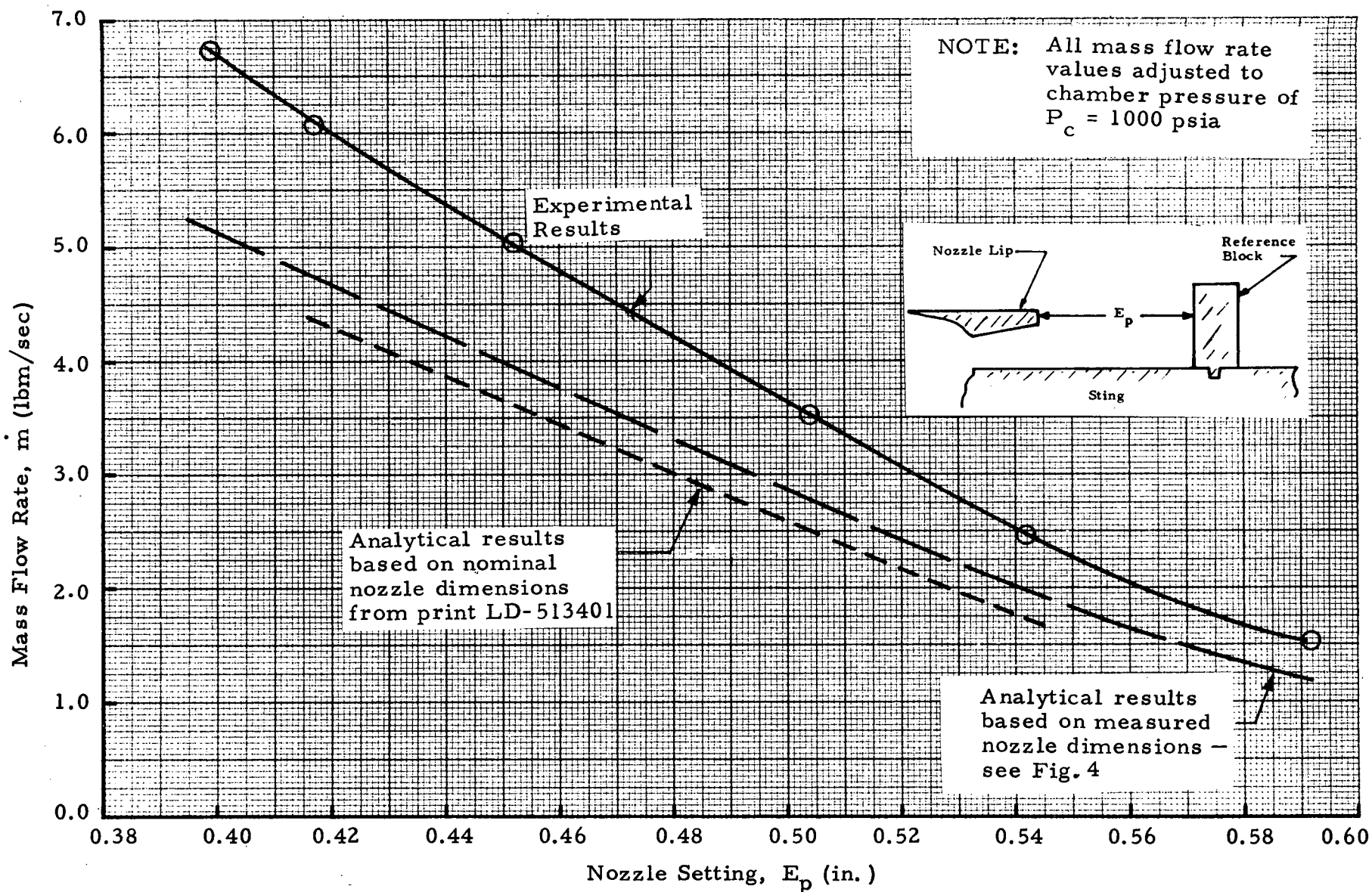


Fig. 8 - Comparison of Experimental and Analytical Mass Flow Rates as a Function of Setting of Booster Nozzle

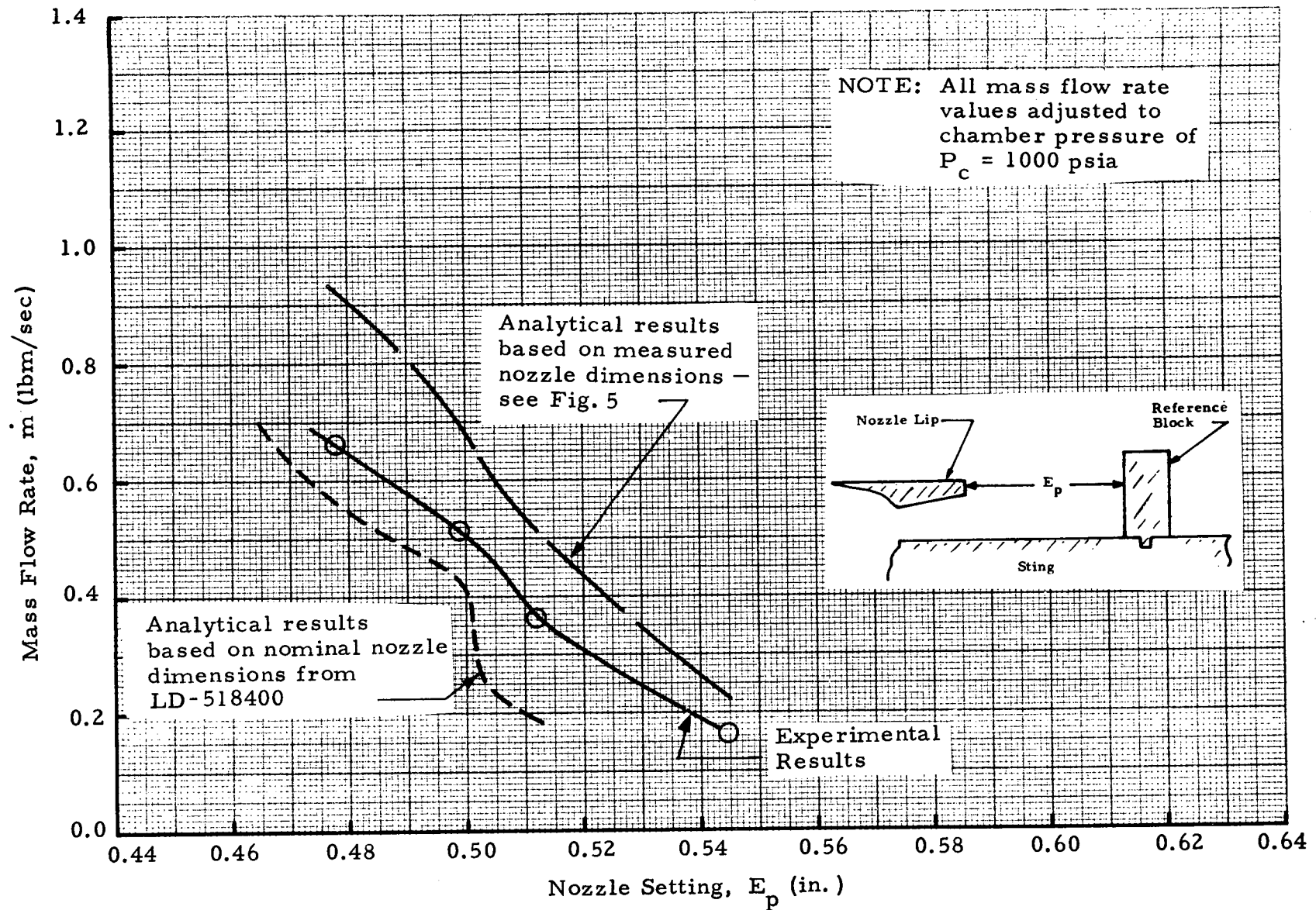


Fig. 9 - Comparison of Experimental and Analytical Mass Flow Rates as a Function of Setting of Orbiter Nozzle

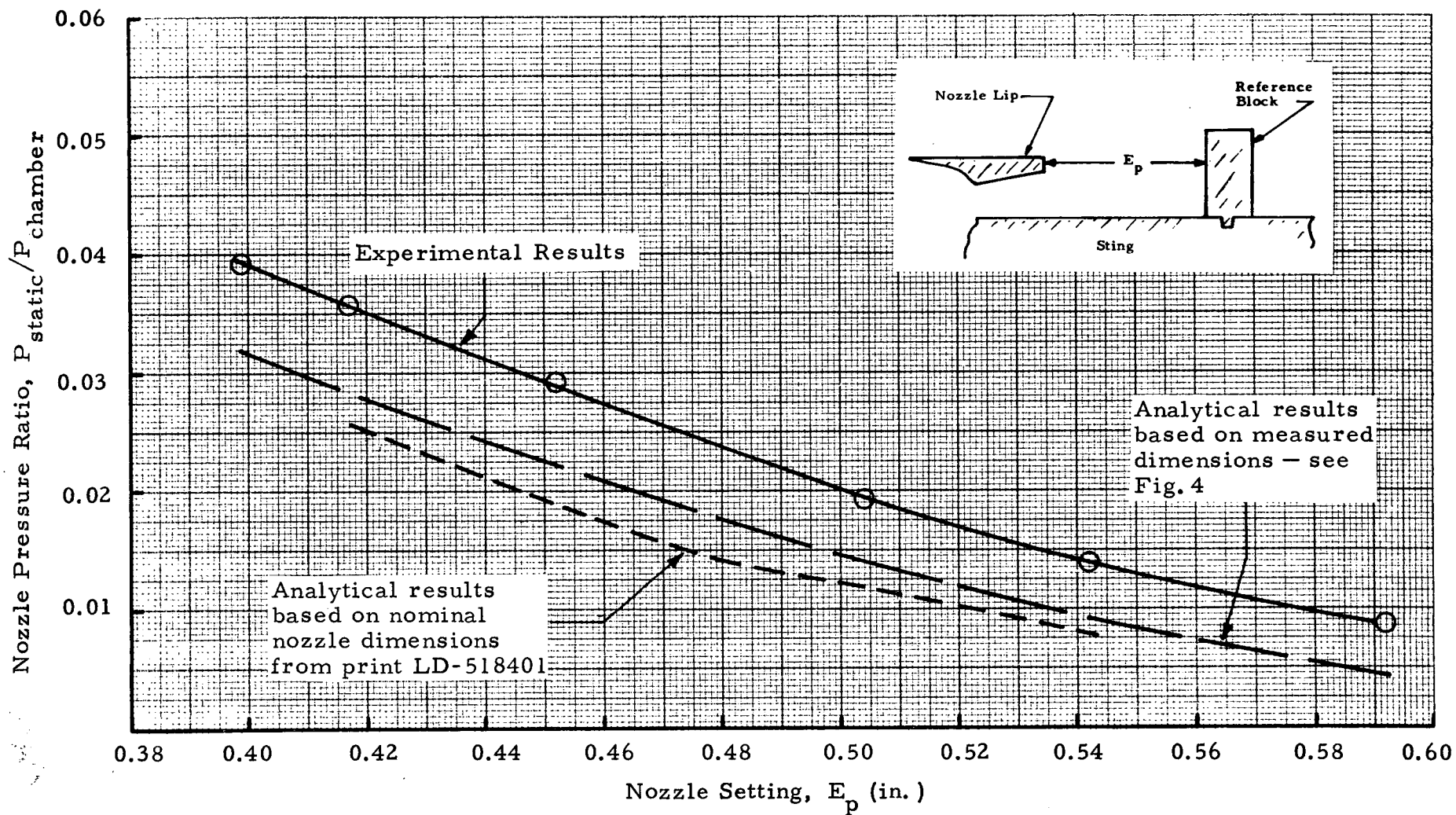


Fig. 10 - Comparison of Experimental and Analytical Nozzle Pressure Ratio as a Function of Setting of Booster Nozzle



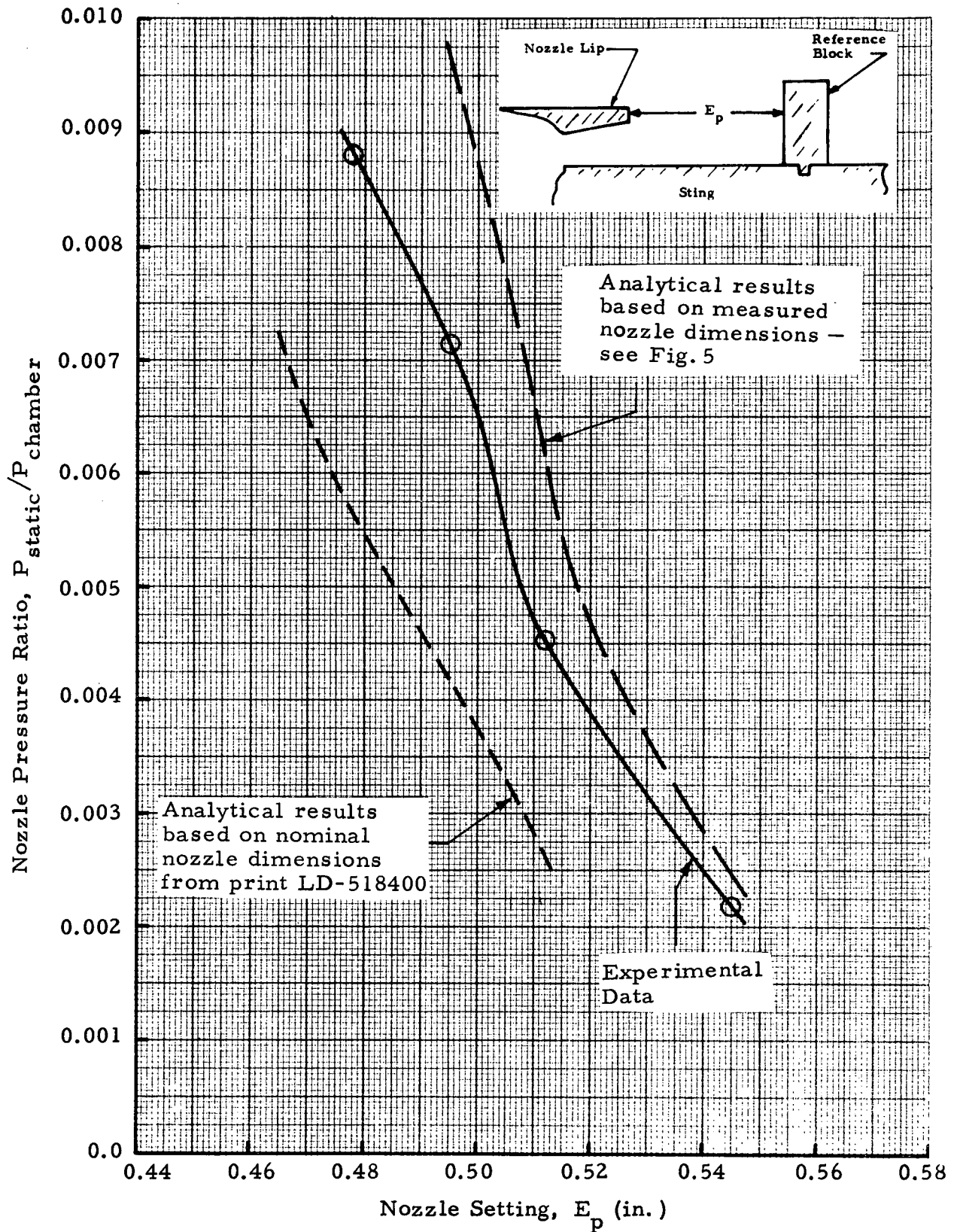


Fig. 11 - Comparison of Experimental and Analytical Nozzle Pressure Ratio as a Function of Setting of Orbiter Nozzle

Reproduced from  
best available copy.

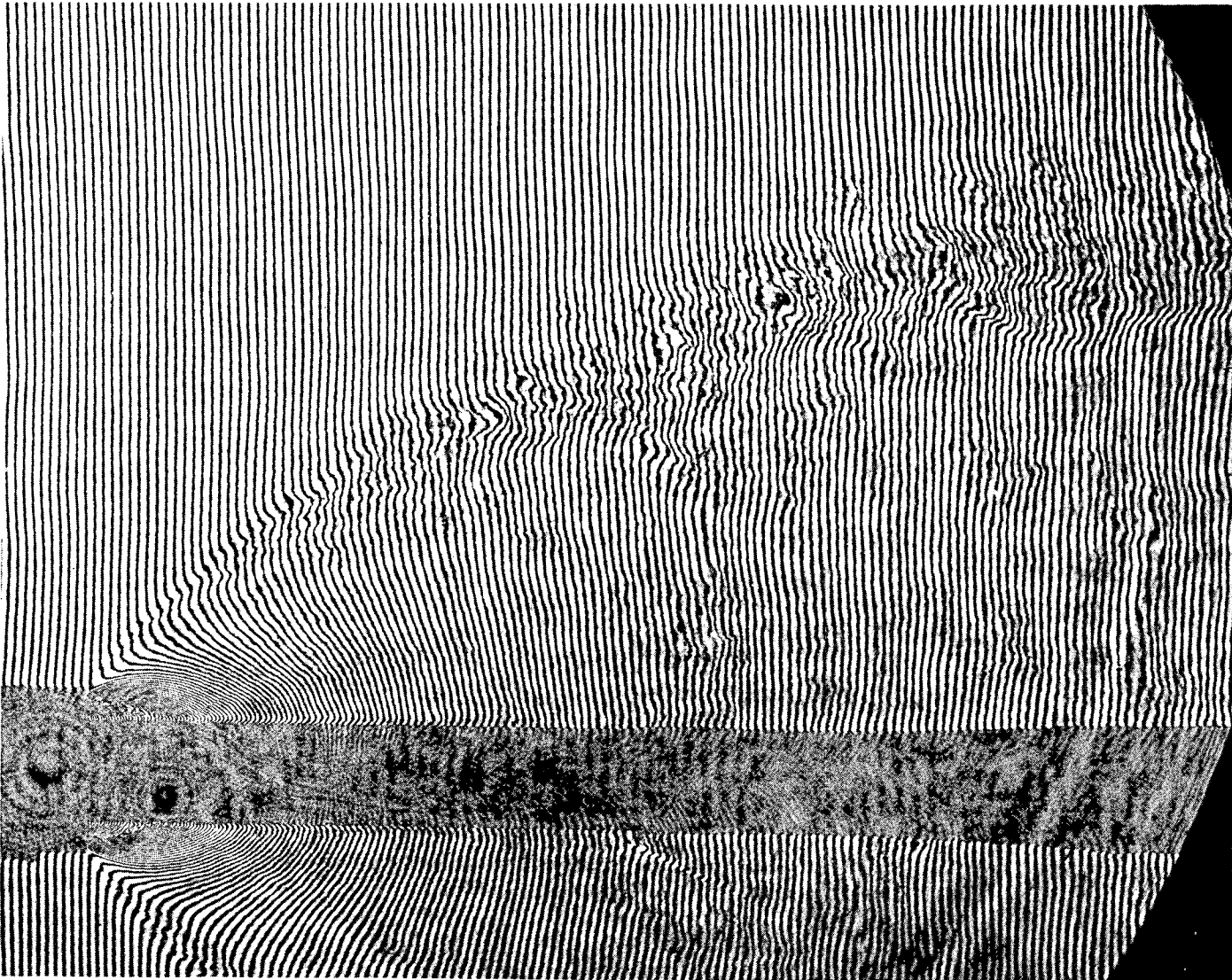


Fig. 12 - Holographic Interferogram of Booster Nozzle Flow

Reproduced from  
best available copy.

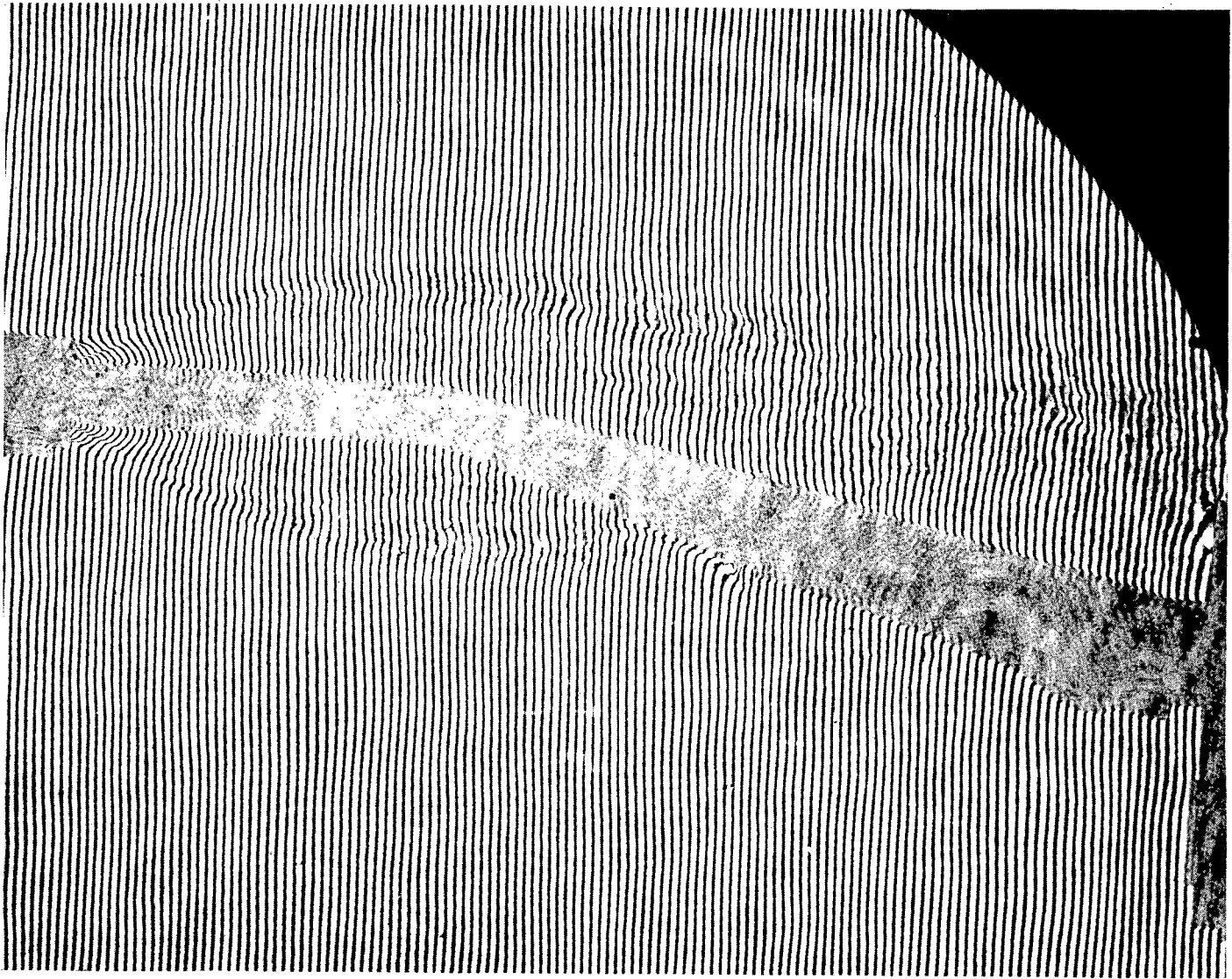


Fig. 13 - Holographic Interferogram of Orbiter Nozzle Flow



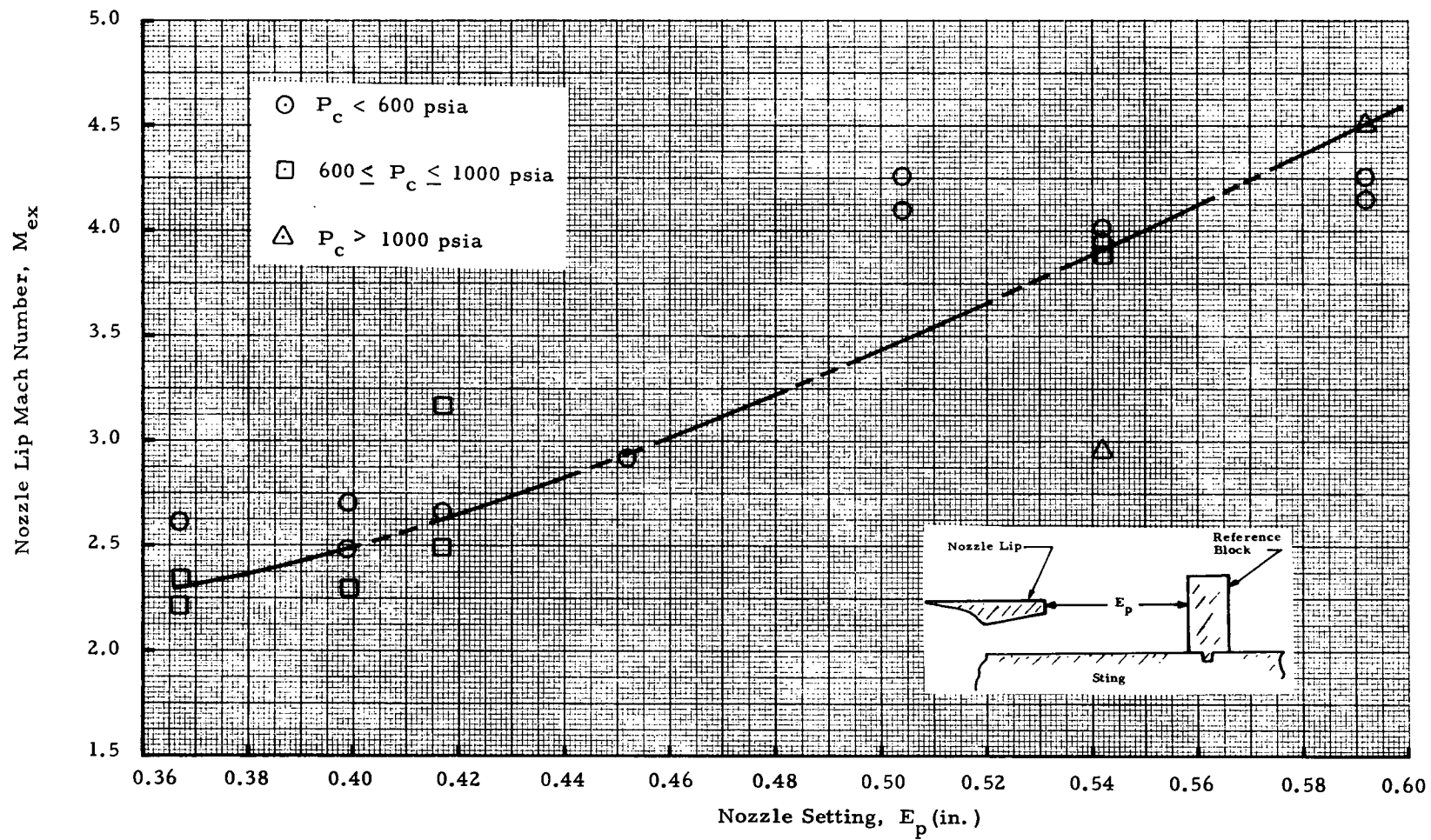


Fig. 14 - Nozzle Exit Lip Mach Number as a Function of Optical Plume Shape Data

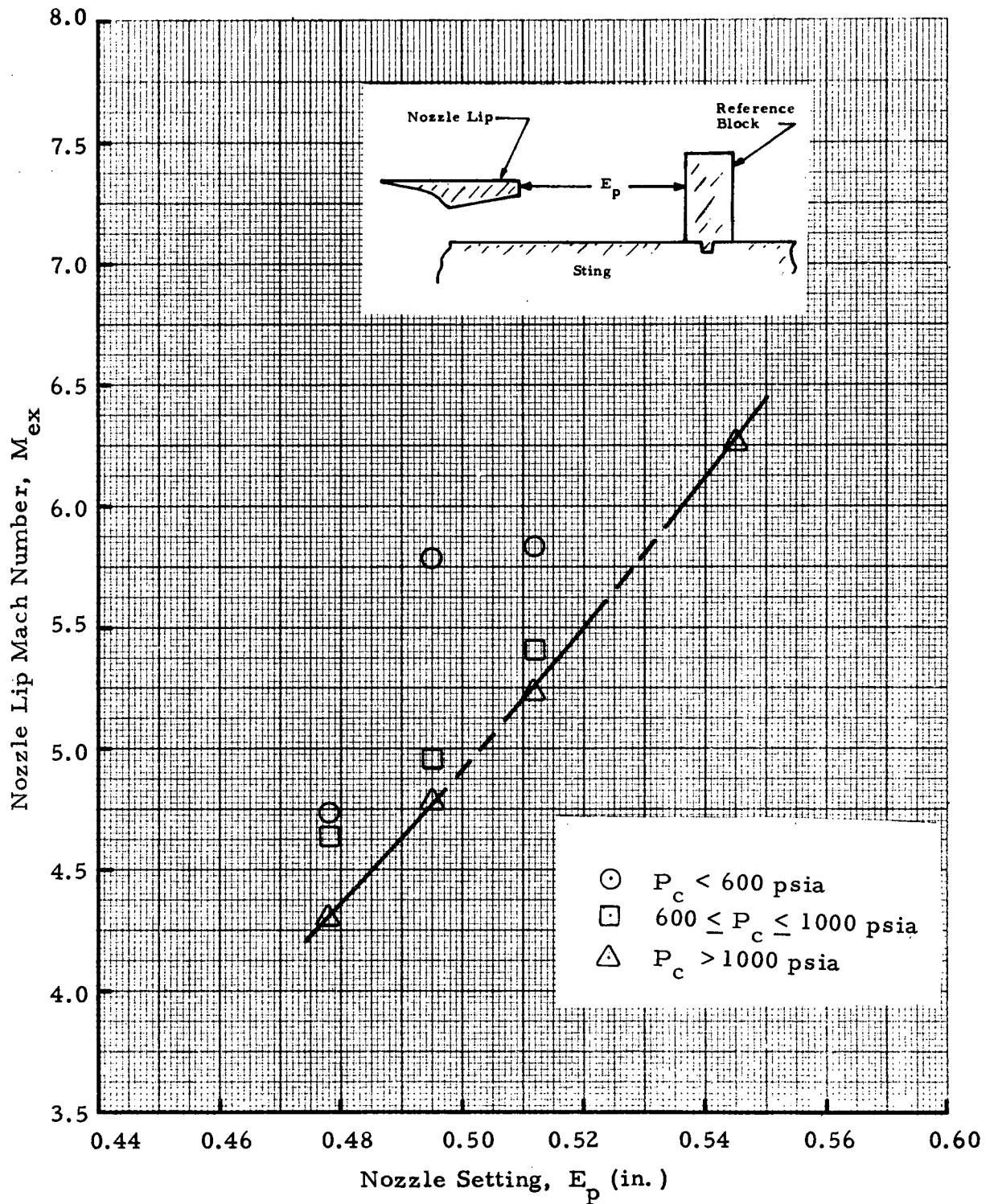


Fig. 15 - Nozzle Exit Lip Mach Number as a Function of Setting of Orbiter Nozzle as Deduced from Optical Plume Shape Data